Apoptosis 2005; **10**: 597–609

Pramanicin induces apoptosis in Jurkat leukemia cells: A role for JNK, p38 and caspase activation

O. Kutuk, A. Pedrech, P. Harrison and H. Basaga

Biological Sciences and Bioengineering Program, Sabanci University, 34956, Tuzla, Istanbul, Turkey (O. Kutuk, H. Basaga); Department of Chemistry, McMaster University, 1280 Main Street West, Hamilton, ON, L8S 4M1, Canada (A. Pedrech, P. Harrison)

Pramanicin is a novel anti-fungal drug with a wide range of potential application against human diseases. It has been previously shown that pramanicin induces cell death and increases calcium levels in vascular endothelial cells. In the present study, we showed that pramanicin induced apoptosis in Jurkat T leukemia cells in a dose- and time-dependent manner. Our data reveal that pramanicin induced the release of cytochrome *c* and caspase-9 and caspase-3 activation, as evidenced by detection of active caspase fragments and fluorometric caspase assays. Pramanicin also activated c-jun N-terminal kinase (JNK), p38 and extracellular signal-regulated kinases (ERK 1/2) with different time and dose kinetics. Treatment of cells with specific MAP kinase and caspase inhibitors further confirmed the mechanistic involvement of these signalling cascades in pramanicin-induced apoptosis. JNK and p38 pathways acted as pro-apoptotic signalling pathways in pramanicin-induced apoptosis, in which they regulated release of cytochrome *c* and caspase activation. In contrast the ERK 1/2 pathway exerted a protective effect through inhibition of cytochrome *c* leakage from mitochondria and caspase activation, which were only observed when lower concentrations of pramanicin were used as apoptosis-inducing agent and which were masked by the intense apoptosis induction by higher concentrations of pramanicin. These results suggest pramanicin as a potential apoptosis-inducing small molecule, which acts through a well-defined JNK- and p38-dependent apoptosis signalling pathway in Jurkat T leukemia cells.

Keywords: caspases; Jurkat; mitogen-activated protein kinases; pramanicin.

Introduction

Pramanicin is a recently discovered potent antifungal agent with a polar head group and an aliphatic side chain (Figure 1). The growth-inhibitory effect of pramanicin on fungal organisms is seen with minimal inhibitory concentrations of 20–100 μM.[1] Pharmacological applications of pramanicin on mammalian systems have not been studied extensively. It has been previously shown that pramanicin increases cytosolic calcium concentrations and induces cell death in endothelial cells,[2] but the effects of pramanicin on cancer cell lines have not been investigated.

The principal aim of all anti-cancer therapies and cancer prevention approaches is to eliminate all tumor cells from the human body. Disequilibrium between cell proliferation and death has been proposed to be a fundamental step in carcinogenesis. Additionally, induction of apoptosis (programmed cell death) is an effective mechanism used to eradicate transformed, deleterious cells; as well, many chemotherapeutic or chemopreventive agents act through triggering of apoptotic pathways in tumor cells. The cellular apoptotic machinery is formed by protein signalling networks, which are finely tuned by protein-protein interactions and protein modifications. The intrinsic and extrinsic apoptotic pathways have been defined previously[3] and protein kinases as well as various cysteinyl-specific aspartate proteases (caspases) have been proposed to mediate apoptosis induced by cytokines, chemotherapeutics and cellular stress through a highly organized network at different signalling levels.[4–6] Briefly, cleavage of initiator caspases (caspase 8 and caspase 9) and the effector caspases (caspase-3/7) and typical cellular features of apoptosis (nuclear condensation and formation of apoptotic bodies) have been observed following the release of cytochrome *c* from mitochondria in response to death receptor stimulation or a direct intracellular insult.

In mammals three distinct groups of mitogen-activated protein kinases (MAPKs) have been identified. c-Jun N-terminal kinases (JNK) and p38 MAPKs have been shown to be activated by cellular stress, UV radiation, growth factor withdrawal and pro-inflammatory cytokines (mainly TNFα and IL-1).[7,8] Upon activation through a dual tyrosine/threonine phosphorylation mechanism by their corresponding upstream kinases, JNK and p38 phosphorylate various transcription factors such as

Correspondence to: Huveyda Basaga, Sabanci University FENS, Biological Sciences and Bioengineering Program, 34956, Tuzla, Istanbul, Turkey. Tel.: +902164839511; Fax: +902164839550; e-mail: huveyda@sabanciuniv.edu

Figure 1. Structure of pramanicin.

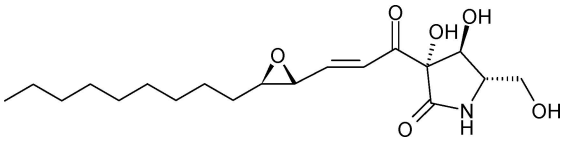

c-jun, ATF-2 and p53 with different substrate specificities and control their transcriptional activity.[9] Both JNK and p38 kinases have been shown to be involved in pro-apoptotic or anti-apoptotic signaling pathways in many different studies.[10,11] However, many stimuli have been shown to activate these kinases without inducing apoptosis.[12–14] The third group of MAPKs, extracellular signal regulated kinases (ERK 1/2, p42/p44 kinases) were demonstrated to be mainly activated by growth factors and other mitogenic stimuli.[15,16] In general, intensive research on MAPKs has suggested that JNKs and p38 are mainly involved in apoptosis and growth arrest, but ERK 1/2 are involved in cellular transformation, differentiation and proliferation. Indeed, the cell type, origin of the stimuli, co-activation of other signalling cascades as well as the initial magnitude, duration and further amplification of the activated signal transduction pathway determine the pro-apoptotic or anti-apoptotic characteristic of the cellular target response. Thus activation patterns and pro-/anti-apoptotic properties of each MAPK should be evaluated carefully in the light of above parameters.

Here we report on the apoptotic effect of pramanicin on Jurkat T lymphoblastic leukemia cells in a dose- and time-dependent manner, as shown by MTT assay and DNA fragmentation. In order to gain insight into the mechanisms of this apoptotic response we followed the activation of MAPKs and caspases in response to pramanicin treatment. Our results have clearly demonstrated the involvement of JNKs and p38 as well as caspase-9 and caspase-3 activation with respect to pramanicin-induced apoptosis in Jurkat T lymphoblastic leukemia cells. Mitochondrial cytochrome *c* is released by pramanicin with similar time-kinetics to caspase-9 activation. Pramanicin also induces an early and transient ERK activation, which contributes to a partial protective effect against apoptosis. To our knowledge, this is the first study that reports pramanicin as a potential novel therapeutic approach against cancer, which acts through an intelligibly JNK- and p38-dependent mechanism.

Materials and methods

Reagents and antibodies

Caspase-3 inhibitor, Z-DEVD-FMK (benzyloxycarbonyl-Asp-Glu-Val-Asp-fluoromethylketone), caspase-9 inhibitor, Z-LEHD-FMK (benzyloxycarbonyl-Leu-Glu-His-Asp-fluoromethylketone) and general caspase inhibitor, Z-VAD-FMK (benzyloxycarbonyl-Val-Ala-Asp-fluoromethylketone) were obtained from BD Biosciences Pharmingen, (San Diego, CA, USA). RPMI 1640 Medium was purchased from Biological Industries, Rehovot, Israel. JNK inhibitor SP600125 (anthra[1,9-cd]pyrazol-6(2H)-one), p38 inhibitor SB203580 (4-(4-fluorophenyl)-2-(4-methylsulfinylphenyl)-5-(4-pyridyl)-1H-imidazole) and MEK1/ERK inhibitor PD98059 (2′-amino-3′-methoxyflavone) were from Calbiochem (San Diego, CA, USA). JNK, phospho-JNK (Thr 183/Tyr 185), p38, phospho-p38, ERK 1/2, phospho-ERK 1/2 and cytochrome *c* antibodies were from Santa Cruz Biotechnology Inc. (Santa Cruz, CA, USA). Caspase-9, caspase-3 and β-actin antibodies were from Cell Signaling Technology Inc. (Beverly, MA, USA). CoxIV (cytochrome c oxidase subunit IV) antibody was purchased from Abcam (Cambridge, UK). Milk Diluent Concentrate Kit was obtained from KPL (Maryland, USA). Phosphatase Inhibitor Cocktail 1, Phosphatase Inhibitor Cocktail 2, digitonin, fetal bovine serum and other chemicals were purchased from Sigma (Darmstadt, Germany) otherwise indicated.

Growth of *Stagonospora* and purification of pramanicin

Stagonospora Sp. ATCC 74253 (American Type Culture Collection, Rockville, MD, USA) was cultured in liquid medium LCM, with the glucose content reduced to 40 g/L (100 mL in each of twelve 500 mL Erlenmeyer flasks). After seven days, the cultures were centrifuged and the supernatant extracted with methyl ethyl ketone. After concentration, the organic extracts were purified by column chromatography (SiO_2, 10% MeOH/EtOAc). Final purification was by MPLC on a Merck LOBAR RP-8 column in MeOH–H_2O (70:30), giving approx. 75 mg of pramanicin, as previously described.[17]

Cell cultures and treatments

Jurkat T lymphoblastic leukemia cells were a kind gift of Dr. Jean-François Peyron, Faculté de Médecine Pasteur, Nice, France and have been previously described.[18] The cells were grown in RPMI-1640 supplemented with 10% fetal bovine serum and penicillin/streptomycin (100 U/mL, respectively) in a humidified incubator at 37°C and 5% CO_2. Cells were seeded in 6-well culture plates (1×10^6cells/well), 60 mm culture flasks (1×10^7 cells/well) or 96-well plates (10^4 cells/well) and treated as indicated in the experimental protocols. Ethanol ($\leq 0.05\%$, v/v) was added to all control wells in each experiment.

Cell viability and DNA fragmentation assays

Cell viability was determined using an MTT assay kit (Roche, Mannheim, Germany) as per the manufacturer's protocol. Briefly, Jurkat cells in 96-well plates were treated as indicated and ten μl of MTT labeling reagent was added to each well, and the plates were incubated for 4 hours. The cells were then incubated in 100 μl of the solubilization solution for 12 hours, and the absorbance was measured with a microtiter plate reader (Bio-Rad, CA, USA) at a test wavelength of 595 nm and a reference wavelength of 690 nm. Percent viability was calculated as (OD of drug-treated sample/control OD) $\times$ 100.

DNA fragmentation was detected as described before with minor modifications.[19] Briefly Jurkat cells (1×10^7 cells/well) were plated on 60 mm culture flasks. After indicated treatments, cells were harvested, washed twice with ice cold PBS and lysed in lysis buffer [10 mM Tris-HCl (pH 8.0), 10 mM EDTA, and 0.2% Triton X-100] on ice for 30 min. Cells were subsequently centrifuged at 13000*g* at 4°C for 10 min; supernatant was collected and transferred to a new tube. Supernatant was incubated with RNase A (200 μg/mL) at 37°C for 1 h and then incubated with Proteinase K (4 mg/mL) with 1.5% SDS solution at 50°C for 2 h. Soluble DNA was isolated by phenol-chloroform-isoamylalcohol extraction and ethanol precipitation. Vacuum dried DNA pellets were dissolved in TE buffer and resolved on 2% agarose gel for 2 h. DNA fragments were visualized by staining with ethidium bromide.

Western blot analysis

Treated and control Jurkat cells were harvested, washed with ice-cold phosphate-buffered saline and lysed on ice in a solution containing 20 mM Tris-HCl (pH 7.5), 150 mM NaCl, Nonidet P-40 0.5%, (v/v), 1 mM EDTA, 0.5 mM PMSF, 1 mM DTT, protease inhibitor cocktail (Complete from Roche, Mannheim, Germany) and phosphatase inhibitors (Phosphatase inhibitor cocktail 1 and 2, Sigma, Darmstadt, Germany). After cell lysis cell debris was removed by centrifugation 10 min at 13000 *g* and protein concentrations were determined with Bradford protein assay. Proteins (40 μg) were separated on a 10–15% SDS-PAGE and blotted onto PVDF membranes. The membranes were then blocked with 5% dried milk in PBS-Tween20 and incubated with appropriate primary and horseradish peroxidase (HRP)-conjugated secondary antibodies (Amersham Pharmacia Biotech, Freiburg, Germany) in antibody buffer containing 10% (v/v) Milk Diluent/Blocking concentrate. After required washes with PBS-Tween 20, proteins were finally analyzed using an enhanced chemiluminescence detection system (ECL-Plus, Amersham Pharmacia Biotech, Freiburg, Germany) and exposed to Hyperfilm-ECL (Amersham Pharmacia Biotech, Freiburg, Germany).

Detection of cytochrome *c* release

Release of cytochrome *c* from mitochondria was detected as described previously.[20] Jurkat cells were seeded in 6-well plates (1×10^6 cells/well) and after indicated treatments, cells were harvested, washed once with phosphate-buffered saline (PBS) and lysed for 30 s in 100 μl ice-cold lysis buffer (250 mM sucrose, 1 mM EDTA, 0.05% digitonin, 25 mM Tris, pH 6.8, 1 mM dithiothreitol (DTT), 0.1 mM PMSF and protease inhibitor cocktail (CompleteMini, Roche, Germany). Cell lysates were centrifuged at 13000 *g* at 4°C for 3 min and supernatants (mitochondria-free cytosolic extracts) and the pellets (mitochondrial fraction) were separately obtained. Cytosolic and mitochondrial fractions were separated on a 15% SDS-PAGE and then analyzed by Western blot using anti-cytochrome *c* antibody and HRP-conjugated secondary antibody. Proteins were finally developed using an ECL-Plus enhanced chemiluminescence detection system and exposed to Hyperfilm-ECL.

Caspase activation assays

The enzymatic activity of caspase-3 and caspase-9 was determined by using a caspase activation assay kit (Sigma, Darmstadt, Germany). Jurkat cells were treated as indicated, washed twice with ice-cold PBS and then resuspended in lysis buffer (250 mM HEPES, pH 7.4, 25 mM CHAPS, 25 mM DTT). After 15 min of incubation on ice, samples were centrifuged for 10 min at 10000 *g* at 4°C, supernatants were collected and protein concentrations were determined by Bradford protein assay. Ten μg of protein were assayed in 200 μl of reaction solution containing Ac-DEVD-AMC for caspase-3-like DEVDase activity and Ac-LEHD-AMC for caspase-9 activity. The released fluorescent AMC was monitored at an excitation of 360 nm and emission of 460 nm using a Spectramax Gemini XS multiplate spectrofluorometer (Molecular Devices, Sunnyvale, CA, USA). Results were calculated from a standard curve of AMC and specific caspase activities were derived as mean relative fluorescence units (RFU)/mg protein. Data shown are mean $\pm$ SEM of three independent experiments performed in triplicate.

Statistical analysis

The results are expressed as mean $\pm$ SEM and the mean values were compared using Students *t*-tail test. Values of $p < 0.05$, $p < 0.01$ and $p < 0.001$ were considered statistically significant.

Results

Pramanicin induces apoptosis in Jurkat cells

In order to investigate the effect of pramanicin on Jurkat cells, we first evaluated the modulation of cell viability using the MTT assay. As demonstrated in Figure 2A, treatment of Jurkat cells with pramanicin significantly affects viability of cells in a dose- and time-dependent manner. Treatment of Jurkat cells with 100 μM pramanicin for 24 h decreases cell viability compared with untreated control ($13.48 \pm 5.11\%$ vs. $97.765 \pm 1.96\%$, $^{***}p < 0.001$). Endonuclease-mediated degradation of chromatin giving rise to DNA laddering is one of the hallmarks of apoptosis. To investigate the effect of pramanicin on DNA laddering, cells were incubated with differing doses of pramanicin for 24 h and 100 μM pramanicin for 0–24 h. Jurkat cells treated with 50 and 100 μM pramanicin contained low molecular weight DNA species that migrated as a ladder (Figure 2B). As well 100 μM pramanicin induces DNA laddering from 12 h after administration (Figure 2C).

Pramanicin induces caspase activation and cytochrome *c* release from mitochondria

To examine the involvement of cytochrome *c* release in pramanicin-induced apoptosis, we evaluated the level of cytochrome *c* in mitochondrial and cytosolic protein fractions by Western blot analysis. Pramanicin treatment at 100 μM concentration induces the release of

Figure 2. Pramanicin induces apoptosis in Jurkat cells in a dose- and time-dependent manner. (A) Jurkat cells were treated with 0–100 μM pramanicin for 0–24 h and after incubation, cell viability was assessed using MTT assay. Results are expressed as means $\pm$ SEM from three independent experiments performed in duplicate. $^{**}p < 0.01$; $^{***}p < 0.001$ compared with untreated sample. (B) Jurkat cells were treated with 0–100 μM pramanicin for 24 h and DNA fragmentation, which indicates apoptosis was detected as described in *Materials and Methods.* C, Jurkat cells were treated with 100 μM for 0–24 h and time-dependency of apoptotic response was evaluated using DNA fragmentation assay as described in *Materials and Methods*.

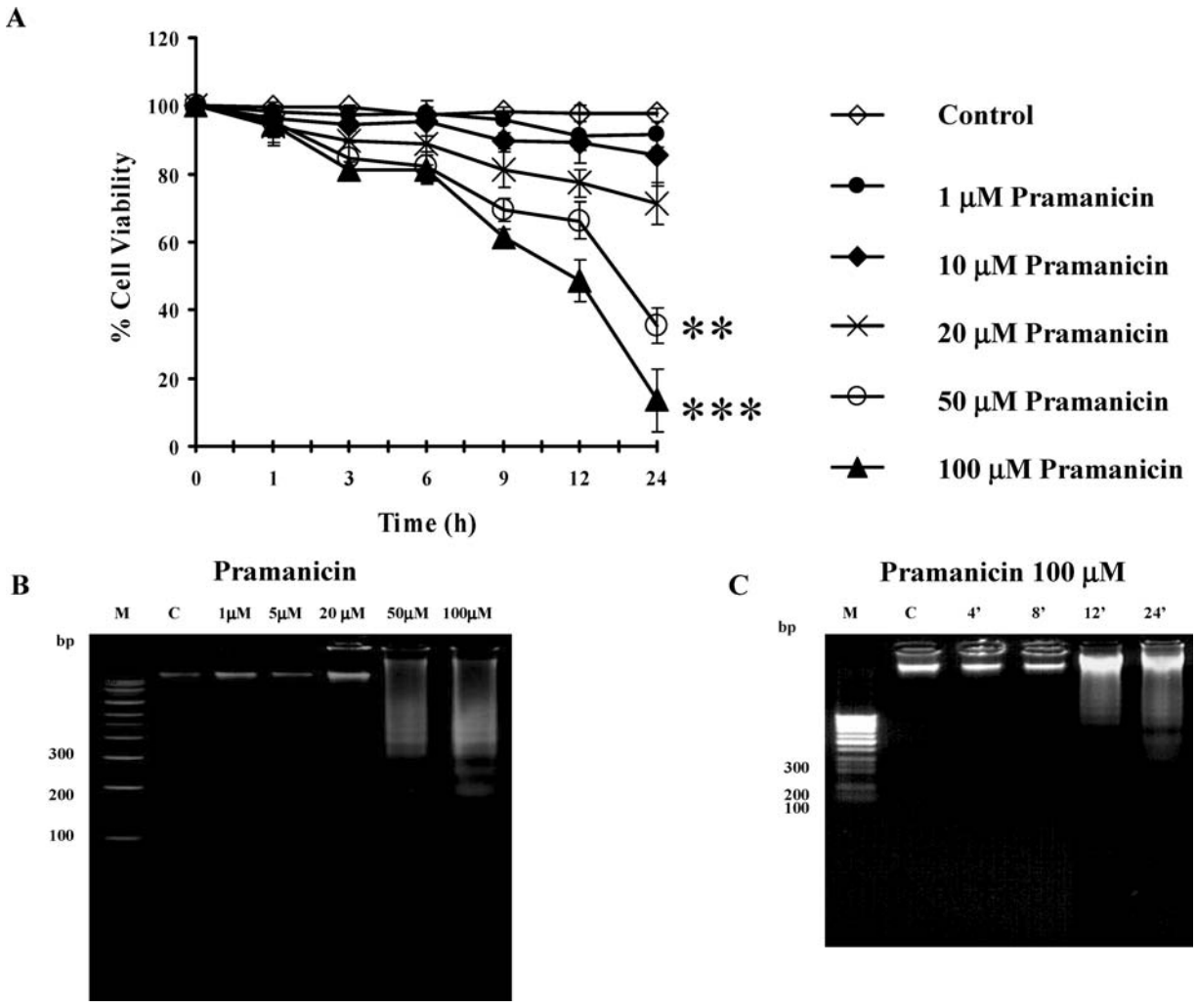

cytochrome *c* from mitochondria and its appearance in the cytosol at 2 h (Figure 3A).

Additionally, Jurkat cells were treated with increasing concentrations of pramanicin and as shown in Figure 3A, cytochrome *c* release from mitochondria is induced in a dose-dependent manner. The release of cytochrome *c* from mitochondria to cytosol results in its binding to Apaf-1 followed by apoptosome formation and caspase-9 activation. The activation status of caspase-9 was assessed in whole cell lysates using immunoblot analysis. Pramanicin (100 μM) induces the processing and appearance of an active caspase-9 intermediate (35 kDa) at 2 h, which is followed by more evident and intense active caspase-9 bands (Figure 3B). Furthermore we followed the dose kinetics of caspase-9 activation by 8 h of pramanicin treatment and as shown in Figure 3B, pramanicin induced caspase-9 activation in a dose-dependent manner with a maximum effect at 100 μM concentration. In parallel, we investigated caspase-9 activation through its ability to cleave its specific substrate (Ac-LEHD-AMC) and formation of the fluorogenic AMC compound. The specificity of the assays was confirmed by inhibitor studies and internal positive controls. As shown in Figure 3B, pramanicin induces the activation of caspase-9 at a dose and with time kinetics similar to results demonstrated by immunoblot analysis, with detection of maximum activation at 100 μM concentration and at 2 h post-treatment.

The death receptor and mitochondrial apoptosis intersect at activation of effector caspases; therefore we analyzed the time and dose kinetics of pramanicin-induced caspase-3 activation in Jurkat cells. Processing of procaspase-3 was evaluated by immunoblotting when cells were treated with pramanicin (100 μM) for 0–8 h and 0–100 μM pramanicin for 8 h. As shown in Figure 3C, pramanicin induced a prominent activation of caspase-3 at 4 h with the appearance of cleaved intermediate products of procaspase-3. This effect was dose-dependent and activation of caspase 3 was evident at 100 μM pramanicin concentration. To further address caspase-3 activity, we also assayed caspase 3-like activity through its ability to cleave the fluorogenic substrate Ac-DEVD-AMC and the release of AMC was monitored as in caspase-9 assays. Pramanicin induces the activation of caspase-3 as shown in Figure 3C, with prominent activation at 100 μM concentration and at 4–8 h post-treatment. The results confirmed the sequential activation of caspase-9 and caspase-3, which indicates an intrinsic mitochondria-mediated signalling pathway in pramanicin-induced apoptosis.

Pramanicin activates JNK, p38 and ERK 1/2 MAP kinases with different kinetics

Many studies have reported the role of MAPKs in apoptosis signalling and potential functional interactions between MAPK and caspase pathways determine the fate of a cell in response to various stimuli. Therefore, we next evaluated pramanicin-induced activation of MAPKs using immunoblot analysis. Pramanicin at 100 μM concentration induced an immediate JNK activation starting from 30 min post-treatment and maximum levels of JNK phosphorylation were observed at 4 and 8 h (Figure 4A, upper panel), without any significant change in JNK protein levels. In addition, we performed concentration-dependent experiments to identify the dose-dependency of JNK activation by pramanicin and treatment of Jurkat cells with pramanicin at different concentrations ranging up to 100 μM for 4 h (Figure 4B, upper panel). As detected by immunoblot analysis of phospho-JNK (p-JNK) proteins, pramanicin induced a dose-dependent activation of the JNK pathway. p38 phosphorylation was also induced at 30 min duration following pramanicin treatment, returning to nearly basal levels at 8 h (Figure 4A, middle panel). Elevation of p38 activation was also dose-dependent with a maximum activation at 100 μM pramanicin concentration (Figure 4B, middle panel). Pramanicin treatment also induced an early, strong but transient phosphorylation of both ERK1 and ERK2 MAP kinases. Interestingly, ERK1 phosphorylation could not be detected after 2 h but we were able to observe phosphorylated ERK2 even at 8 h after pramanicin treatment (Figure 4A, lower panel). To evaluate the dose-dependent activation of the ERK 1/2 pathway by pramanicin, we also followed the phosphorylated and active ERK 1/2 proteins by means of immunoblot analysis. As shown in (Figure 4B, lower panel), pramanicin treatment induced activation of both the ERK1 and ERK2 in a dose-dependent manner with respect to untreated control cells, but the maximum activation of the ERK 1/2 pathway was detected at 50 μM pramanicin concentration. These findings demonstrate that pramanicin is able to induce the activation of all three MAPKs with different time kinetics and characteristics. Thus, it was of interest to further evaluate the crosstalk between caspase and MAP kinase activation cascades as well as the specific involvement of each pathway in pramanicin-induced apoptosis.

MAP kinases and caspases are functionally involved in pramanicin-induced apoptosis

Activation of MAP kinases either upstream or downstream of mitochondria-mediated caspases activation has been demonstrated to regulate apoptosis in various experimental models. Therefore, we investigated whether activated MAP kinases and caspases are involved in pramanicin-involved apoptosis. To evaluate the involvement of JNK, p38 and ERK 1/2, Jurkat cells were treated with pramanicin for 24 h in the absence and presence of specific MAP kinase inhibitors and the apoptotic response was evaluated by MTT and DNA fragmentation assays.

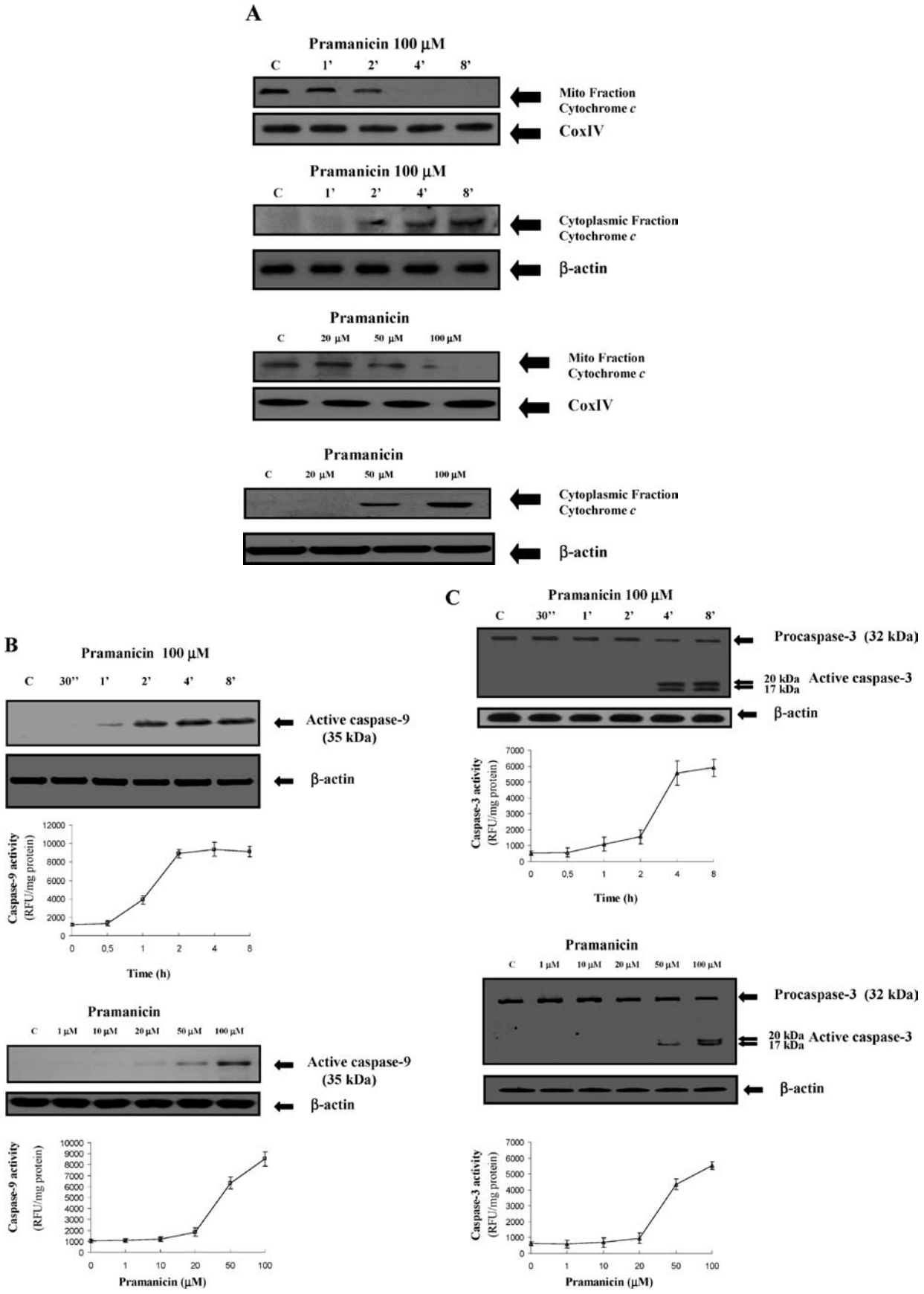
A
Pramanicin 100 μM
C 1' 2' 4' 8'
Mito Fraction Cytochrome c
CoxIV
Pramanicin 100 μM
C 1' 2' 4' 8'
Cytoplasmic Fraction Cytochrome c
β-actin
Pramanicin
C 20 μM 50 μM 100 μM
Mito Fraction Cytochrome c
CoxIV
Pramanicin
C 20 μM 50 μM 100 μM
Cytoplasmic Fraction Cytochrome c
β-actin
B
Pramanicin 100 μM
C 30'' 1' 2' 4' 8'
Active caspase-9 (35 kDa)
β-actin
Caspase-9 activity (RFU/mg protein)
Time (h)
Pramanicin
C 1 μM 10 μM 20 μM 50 μM 100 μM
Active caspase-9 (35 kDa)
β-actin
Caspase-9 activity (RFU/mg protein)
Pramanicin (μM)
C
Pramanicin 100 μM
C 30'' 1' 2' 4' 8'
Procaspase-3 (32 kDa)
20 kDa 17 kDa Active caspase-3
β-actin
Caspase-3 activity (RFU/mg protein)
Time (h)
Pramanicin
C 1 μM 10 μM 20 μM 50 μM 100 μM
Procaspase-3 (32 kDa)
20 kDa 17 kDa Active caspase-3
β-actin
Caspase-3 activity (RFU/mg protein)
Pramanicin (μM)

Figure 3. Pramanicin induces mitochondrial cytochrome *c* release and caspase activation in Jurkat cells. (A) Jurkat cells were treated with 100 μM pramanicin for 0–8 h (upper panels) or treated with 0, 20, 50 and 100 μM pramanicin for 8 h (lower panels). Following indicated incubations, mitochondrial and cytoplasmic fractions of cytochrome *c* were detected by immunoblot analysis. CoxIV and β-actin were probed as a loading control for mitochondrial and cytoplasmic fractions respectively. Results are representative of three independent experiments. (B) Jurkat cells were treated with 0–100 μM pramanicin for 8 h (upper panels) or 100 μM pramanicin for 0–8 h (lower panels) and the activation of caspase-9 was evaluated by immunoblot analysis (performed by using a specific antibody against active caspase-9) and fluorometric caspase assays. In caspase assays, results were expressed as mean $\pm$ SEM from three independent experiments performed in triplicate. (C) to examine the activation of caspase-3, Jurkat cells were treated with 0–100 μM pramanicin for 8 h (upper panels) or 100 μM pramanicin for 0–8 h (lower panels) and the activation of caspase-3 was evaluated by immunoblot analysis (performed by using a specific antibody against procaspase-3 and active caspase-3 fragments) and fluorometric caspase assays. β-actin was probed as a loading control for immunoblots. In caspase assays, results were expressed as mean $\pm$ SEM from three independent experiments performed in triplicate.

Figure 4. Pramanicin activates MAP kinases with different time- and dose-kinetics. A, Jurkat cells were treated with 100 μM pramanicin for 0–8 h and total proteins were isolated. Activities of JNKs, p38 and ERK 1/2 MAP kinases were detected by immunoblot analysis. Specific antibodies against total and phospho-JNKs (upper panel), total and phospho-p38 (middle panels) and total and phospho-ERK 1/2 (lower panels) were used for immunoblot analyses. B, for dose-dependent MAP kinase activation Jurkat cells were treated with 0–100 μM pramanicin for 4 h to detect JNK activation (upper panels), 2 h for p38 activation (middle panels) and 30 min for ERK 1/2 (lower panels) activation. Total proteins were isolated and analyzed by means of immunoblot. Specific antibodies were used to detect total and phospho-MAP kinases as described above. β-actin was probed as a loading control for immunoblots and results are represententative of three independent experiments.

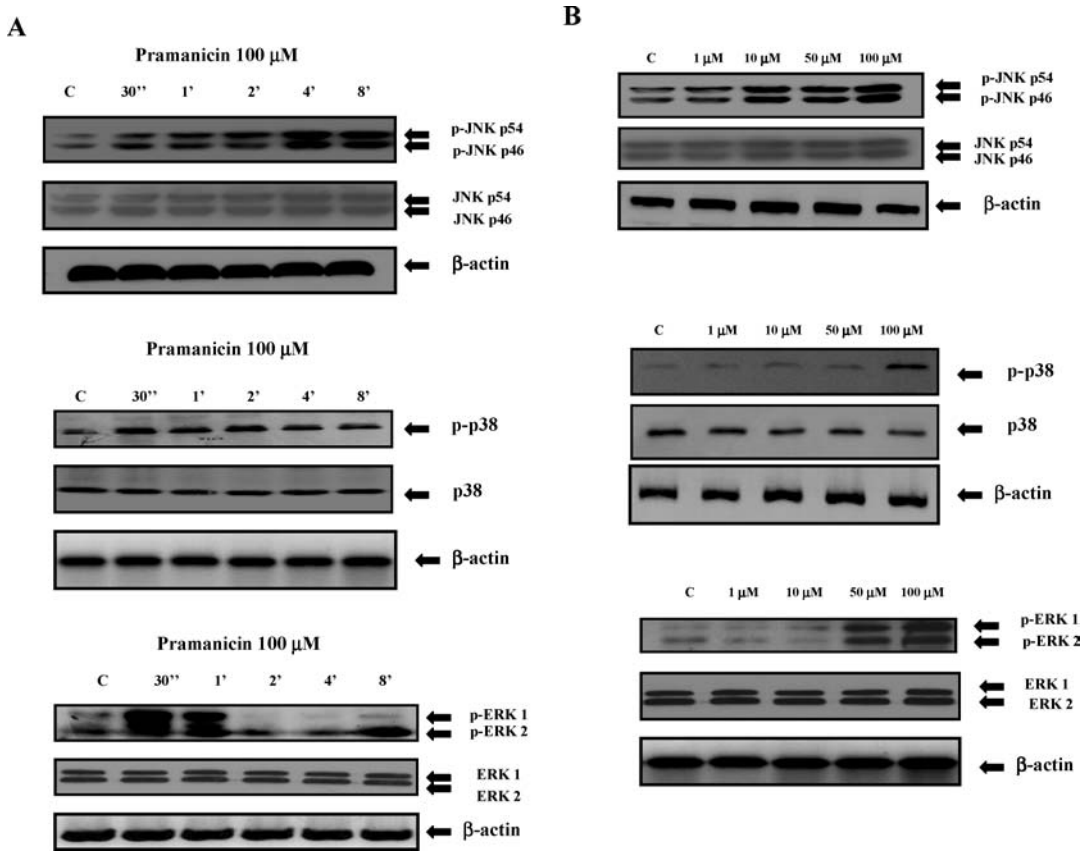

As shown in Figures 5A and B, Lanes 7, JNK inhibitor (SP600125) at 10 μM concentration significantly protects Jurkat cells against pramanicin-induced apoptosis ($^{***}p < 0.001$, compared to pramanicin (100 μM) treated cells). p38 inhibitor (SB203580) at 10 μM concentration also abrogated pramanicin-induced apoptosis ($^{***}p < 0.001$, compared to pramanicin (100 μM) treated cells) (Figures 5A and B, Lanes 6).

ERK inhibitor (PD98059) does not have any significant effect on pramanicin-induced apoptosis at 100 μM concentration (Figures 5A and B, Lanes 3), but interestingly PD98059 enhances pramanicin-induced apoptosis of Jurkat cells at 50 μM concentration ($^{\S}p < 0.05$, compared to pramanicin (50 μM) treated cells) (Figures 5A and B, Lanes 4 and 5 respectively). These results suggest that activation of JNK and p38 pathways are necessary

Figure 5. Effects of MAP kinase and caspase inhibitors on pramanicin-induced apoptosis in Jurkat cells. Jurkat cells were pretreated with specific MAP kinase and caspase inhibitors (10 μM ERK inhibitor (PD98059), 10 μM p38 inhibitor (SB203580) and 10 μM JNK inhibitor (SP600125) for 1 h; 20 μM pancaspase inhibitor (z-VAD-FMK), 20 μM Caspase-9 inhibitor (z-LEHD-FMK) and 20 μM Caspase-3 inhibitor (z-DEVD-FMK) for 30 min) which is followed by 100 or 50 μM pramanicin treatment for 24 h. Untreated negative controls and cells treated with 100 or 50 μM pramanicin without inhibitor pre-treatment were also involved in experimental panels. The lanes for specific treatments are indicated in the figure. After incubation, the effects of specific kinase and caspase inhibitors on pramanicin-induced apoptosis were evaluated by A, DNA fragmentation and B, MTT cell viability assay as described in *Materials and Methods*. MTT results are expressed as means ± SEM from three independent experiments performed in duplicate. * $p < 0.01$; ** $p < 0.001$ compared with 100 μM pramanicin- treated sample. § $p < 0.05$, compared with 50 μM pramanicin-treated sample.

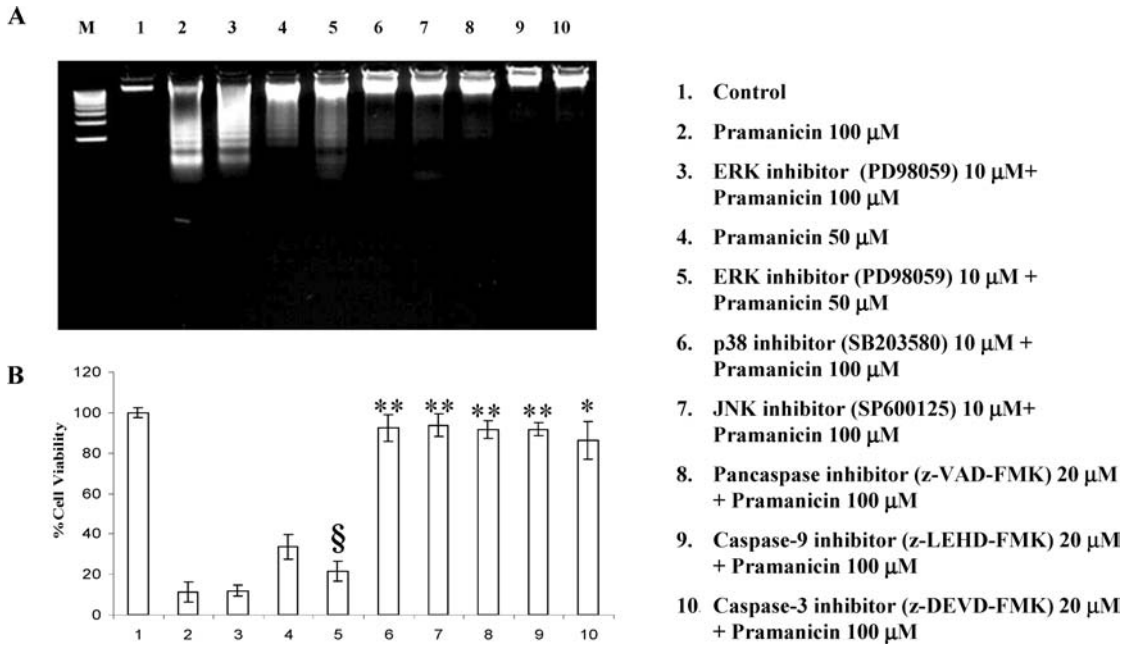

for pramanicin-induced apoptotic response, but ERK 1/2 has a potential pro-survival role.

To determine the functional involvement of caspases in pramanicin-induced apoptosis, we incubated Jurkat cells with pancaspase inhibitor (z-VAD-FMK), caspase-9 inhibitor (z-LEHD-FMK) and caspase-3 inhibitor (z-DEVD-FMK) in the absence or presence of pramanicin (100 μM) and then the apoptotic response was assessed using MTT and DNA fragmentation assays. As shown in Figures 5A and B, Lanes 8 pancaspase inhibitor prevents pramanicin-induced apoptosis. As well, caspase-9 inhibitor (Figures 5A and B, Lanes 9) and caspase-3 inhibitor (Figures 5A and B, Lanes 10) show a protective effect against pramanicin-induced apoptosis. These results confirm that pramanicin triggers a pro-apoptotic pathway in Jurkat cells, which involves MAP kinases and caspases.

JNK and p38 pathways regulate cytochrome *c* release and caspase activation in pramanicin-treated Jurkat cells

In order to clarify the functional mechanisms by which MAP kinases and caspases regulate pramanicin-induced apoptosis, we tried to identify the mechanistic relationship between two pathways. As a starting point, we pretreated Jurkat cells with JNK inhibitor (SP600125) for 1 h before pramanicin (100 μM) treatment for 8 h and followed cytochrome *c* release from mitochondria and caspase-9 and caspase-3 activation by means of immunoblot analysis and caspase activation assays. JNK inhibitor (SP600125) prevented pramanicin-induced release of cytochrome *c*, caspase-9 and caspase-3 activation (Figure 6A). Caspase activation assays confirm the inhibitory effect of JNK inhibitor. In contrast, caspase inhibitors do not have any effect on JNK activation by pramanicin pretreatment (results not shown).

Following characterization of JNK-caspase pathway crosstalk, we pretreated the cells with p38 inhibitor (SB203580) for 1 h before pramanicin (100 μM) treatment and we evaluated cytochrome *c* release and activation of caspases. As shown in Figure 6B, inhibition of the p38 abrogates the release of cytochrome *c*, as well as the activation of caspase-9 and caspase-3 in response to pramanicin treatment. Caspase activation assays also confirmed that the inhibition of the p38 pathway counteracted the pramanicin-induced caspase activation. Again, caspase inhibitors showed no effect on p38 activation by pramanicin (results not shown). The results presented in

Figure 6. Effects of MAP kinase inhibitors on pramanicin-induced cytochrome *c* release and caspase activation in Jurkat cells. Jurkat cells were pretreated with or without A, 10 μM JNK inhibitor (SP600125) B, 10 μM p38 inhibitor (SB203580) C, 10 μM ERK inhibitor (PD98059) for 1 h and then treated with 100 μM pramanicin for 8 h. Cells were either fractioned into cytosolic or mitochondrial extracts to detect cytochrome *c* release or total proteins were isolated to follow caspase-9 and caspase-3 activation by means of immunoblot analysis as described in *Materials and Methods*. β-actin was probed as a loading control for all immunoblots. Fluorometric caspase activation assays were also conducted to confirm active caspase immunoblots. D, Jurkat cells were pretreated with or without 10 μM ERK inhibitor (PD98059) for 1 h and then treated with 50 μM pramanicin for 8 h. Cytochrome *c* release and activation of caspases were detected as described above. Results of caspase activation assays are expressed as mean $\pm$ SEM from three independent experiments performed in triplicate. (*Continued on next page*.)

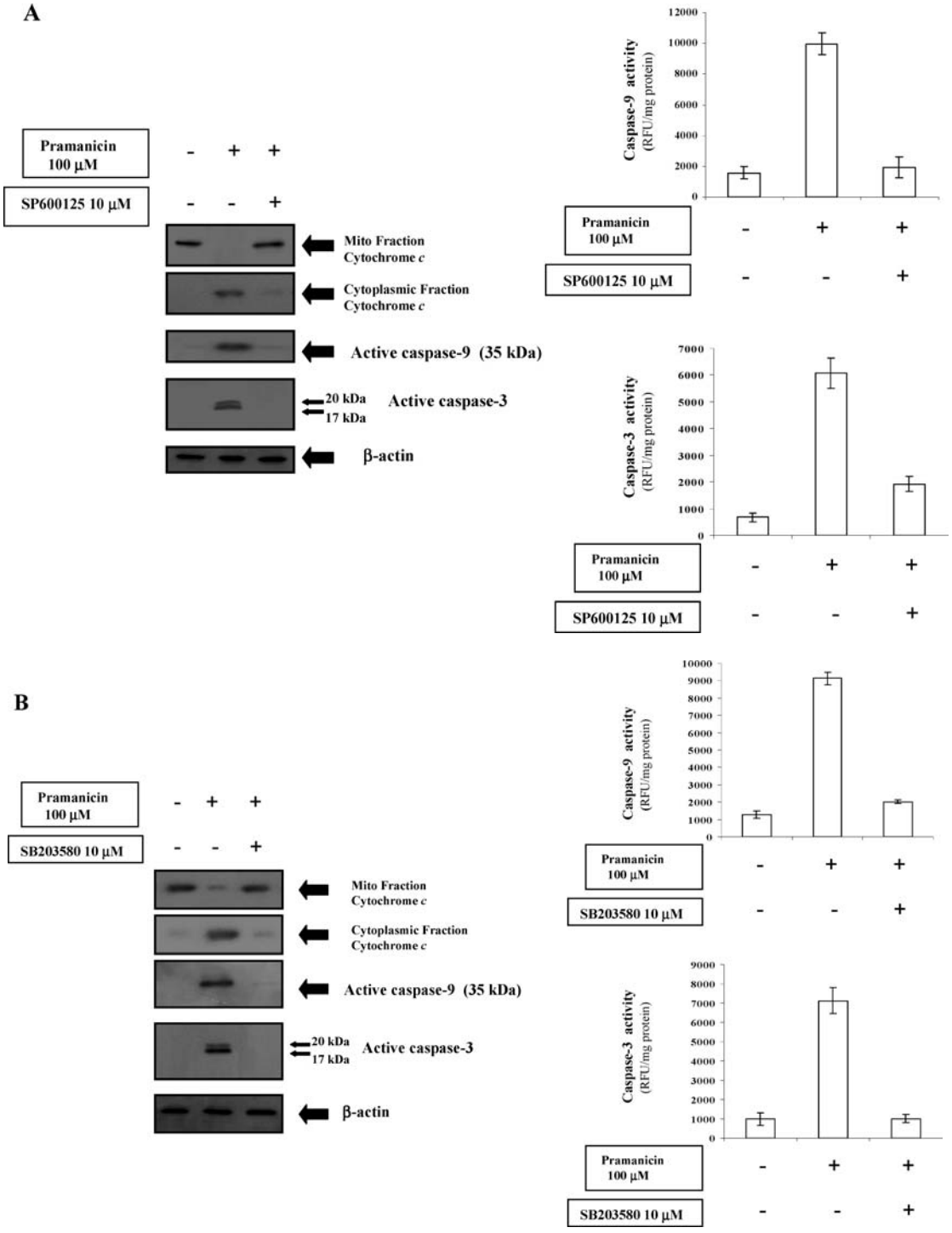

Figure 6. (*Continued*).

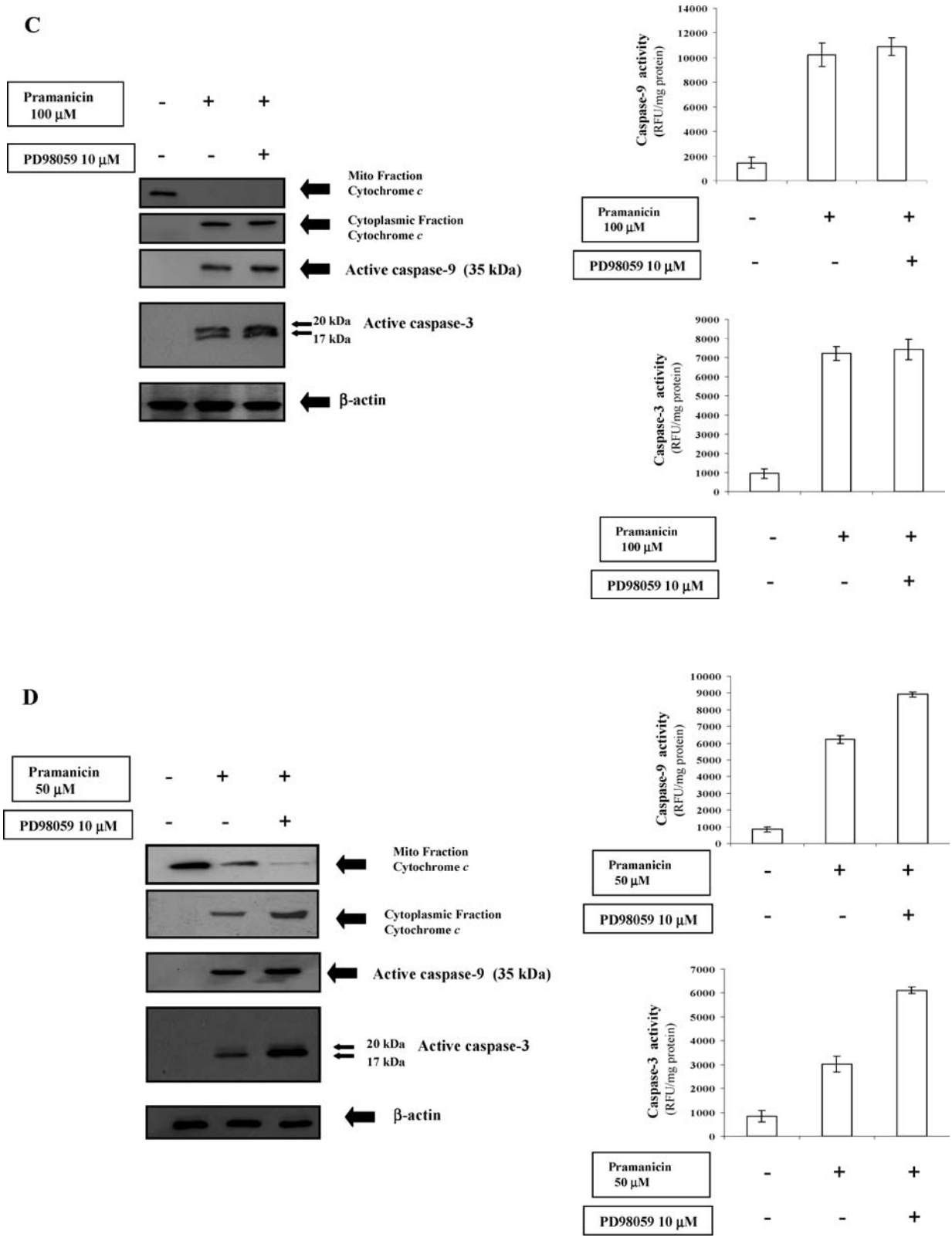

Figure 5A and B indicate a pro-survival role for ERK 1/2 MAP kinase pathway. Therefore, we further investigated the effect of the ERK 1/2 pathway on caspase activation and mitochondrial cytochrome *c* release and as seen in Figure 6C, incubation of Jurkat cells with ERK 1/2 inhibitor (PD98059) for 1 h before treatment with pramanicin (100 μM) does not have any prominent effect on cytochrome *c* release and caspase activation. But PD98059 pretreatment potentiates cytochrome *c* release, caspase-9 and caspase-3 activation by lower concentrations of pramanicin (50 μM) (Figure 6D). The caspase inhibitors did not show any significant effect on ERK1/2 activation by pramanicin pretreatment (results not shown). In summary, these findings indicate that JNK and p38 mediate pramanicin-induced activation of the mitochondrial apoptotic machinery, acting upstream of mitochondria. Additionally the ERK1/2 pathway also acts upstream of mitochondria and exerts a pro-survival role in pramanicin-induced apoptosis signalling, but its effects can be observed at lower concentrations of pramanicin and the potential anti-apoptotic properties of ERK1/2 activation are masked by strong pro-apoptotic signalling triggered by pramanicin at high concentrations.

Discussion

Novel strategies in cancer prevention, diagnosis and treatment have been the subject of intense research for decades. The recognition of apoptosis as a powerful defense mechanism against carcinogenesis and as a target for tumor destruction approaches reshaped cancer research and the apoptotic machineries that are composed of signalling networks with modules of protein kinases, adaptor proteins and secondary messengers have been identified.[21] After all, many chemotherapeutic agents which are already utilized in cancer treatment have been shown to target intra- and extra-cellular signalling cascades and thereby enforce pre-malignant or malignant cells to activate their programmed cell death machineries.[22–24] Identification of key players in apoptotic signalling enables researchers to design small molecule approaches, peptide-based therapeutic regimens and novel adjuvant agents for effective and safe cancer treatment protocols.

Pramanicin is a novel antifungal agent, which was isolated from a sterile fungal fermentation of *Stagonospora* and it was shown to exert a potent growth inhibitory effect on fungal organisms with minimal inhibitory concentrations of 20–100 μM.[1]Harrison *et al.* characterized the biosynthesis of pramanicin.[25] Although pramanicin has been assumed to have potential application opportunities, research on its pharmacological and molecular properties on different experimental models have only started recently. It has been previously shown that pramanicin causes NO-mediated and endothelium-dependent vascular relaxation as well as a transient peak in cytosolic Ca^{2+} concentration and cell death in vascular endothelial cells.[2] Therefore, we investigated the potential apoptotic effect of pramanicin on Jurkat T lymphoblastic leukemia cells and the signalling mechanisms involved in the process.

Our results demonstrated that pramanicin treatment induces apoptosis in Jurkat cells in a dose- and time-dependent manner. Pramanicin at 100 μM concentration efficiently induced apoptosis in Jurkat cells and after characterization of kinetics in pramanicin-induced apoptosis, we then tried to identify the mechanisms involved in this apoptotic process. The release of cytochrome *c* is essential for apoptosome formation and caspase-9 activation as a part of intrinsic apoptosis signalling. Activated caspase-9 then targets downstream effector caspases, such as caspase-3 and the activated effector caspases target intracellular proteins for cleavage and promote the progress of programmed cell death. Here we show that pramanicin leads to the release of cytochrome *c* from mitochondria and caspase-9 and caspase-3 activation with kinetics similar to that for induction of apoptosis. These findings indicated a mitochondria-dependent apoptotic signalling pathway in pramanicin-induced apoptosis.

Protein kinases are the enzymes that catalyze the phosphorylation of specific target proteins in response to intracellular or extracellular stimuli. MAP kinases are members of an evolutionarily conserved protein family from yeast to complex eukaryotic organisms.[7,8] MAP kinases regulate essential cellular functions such as proliferation, cell cycle progression, gene expression and apoptosis and any deregulation or over activity in the phosphorelay system of MAP kinases may lead to human pathologies such as cancer, neurodegenerative diseases and autoimmune disorders.[26–28] There are three main subgroups of MAP kinases that have been defined in mammalian systems: JNK, ERKs and p38 MAP kinases. Activation of JNK and/or p38 protein kinases has been shown to play a critical role in programmed cell death in response to UV and γ-ray radiation, serum deprivation, chemotherapeutics and pro-inflammatory cytokines; although some research groups reported that in other instances they act either as pro-survival signals or remain unrelated to the apoptotic process.[10,11,29–31] Furthermore some reports suggested that active ERK1/2 signaling pathways may inhibit Fas-mediated apoptosis in T-cells and in contrast ERK1/2 has been suggested to exert a pro-apoptotic effect in regulation.[32,33] Therefore, it can be an oversimplification to strictly identify these kinases pro- or anti-apoptotic and ongoing extensive research on the functional properties of MAP kinases indicate that pro-apoptotic or anti-apoptotic actions of these kinases depend on the cell type, duration and amplitude of activation and the presence of other agonists/antagonists. Our results indicate that pramanicin leads to activation of all three MAP kinases, but with different time kinetics and amplitudes. Pramanicin

(100 μM) led to an early activation of p38 and a gradual increase of p-JNK levels which reached a maximum at 4 h; as well an early but transient ERK 1/2 activation was also induced. An interesting finding which was derived from dose-dependent activation patterns of MAP kinases by pramanicin was that activation of JNK and p38 kinases was induced maximally at 100 μM pramanicin concentration, but a maximal activation of ERK 1/2 could be reached even at 50 μM pramanicin concentration. The involvement of activated caspases and MAP kinases in pramanicin-induced apoptosis was evaluated using their specific inhibitors. Caspase inhibitors successfully inhibited the pramanicin-induced apoptotic response and revealed the functional involvement of the caspase pathway. Pretreatment with JNK inhibitor (SP600125), p38 inhibitor (SB203580) and caspase inhibitors effectively prevented the apoptosis induced by 100 μM pramanicin. To our surprise, ERK inhibitor (PD98059) pretreatment did not have any significant effect on the apoptosis induced by 100 μM pramanicin, but it potentiated the apoptotic response of Jurkat cells to 50 μM pramanicin. All these data indicate the functional apoptotic involvement of the p38 and JNK pathways and an anti-apoptotic role for the ERK 1/2 pathway, which was masked by the strong apoptotic response at higher concentrations of pramanicin but became important at lower concentrations of pramanicin treatment. To further establish the molecular mechanisms of this differential MAP kinase involvement in pramanicin-induced apoptosis, we investigated the release of cytochrome *c* and caspase-9 and caspase-3 activation by utilizing pretreatments with specific MAP kinase inhibitors before pramanicin stimulation. As expected pretreatment with JNK inhibitor (SP600125) and p38 inhibitor (SB203580) prevented cytochrome *c* release and caspase activation by 100 μM pramanicin and ERK inhibitor (PD98059) showed no effect. Moreover, pretreatment with ERK inhibitor (PD98059) leads to a more pronounced release of cytochrome *c* and caspase activation by 50 μM pramanicin, which explains the enhancement of apoptotic response of Jurkat cells to 50 μM pramanicin after pretreatment with ERK inhibitor (PD98059). The caspase inhibitors did not show any effect on MAP kinase activation patterns. These findings suggest that MAP kinases act upstream of caspases and they act on mitochondria to control the apoptosis in response to pramanicin treatment, either in a provocative manner as in the case of p38 and JNK or in an inhibitive manner as in the case of ERK 1/2.

In conclusion, we report here on the activation of an apoptotic signaling pathway by a novel antifungal agent; pramanicin, which involves the activation of JNK/p38 kinase cascades, mitochondrial cytochrome *c* release and caspase-9/3 activation. ERK 1/2 activation can counteract the apoptosis induced by pramanicin only at lower concentrations of drug-treatment through inhibition of cytochrome *c* leakage and caspase activation. Altogether these results strongly suggest pramanicin as a potential apoptosis-inducing pharmacological agent in Jurkat cells and studies focusing on different cancer cell lines and/or experimental animal models will further extend our understanding of mechanisms involved in apoptotic response to pramanicin and will allow us to better evaluate the anti-cancer potential of this molecule.

Acknowledgment

This work was supported by Sabanci University Research Funds. P. Harrison thanks the Natural Sciences and Engineering Research Council of Canada (NSERC) for a discovery grant.

References

1. Schwartz RE, Helms RG, Bolessa EA, *et al.* Pramanicin, a novel antimicrobial agent from a fungal fermentation. *Tetrahedron* 1994; **50**: 1675–1686.
2. Kwan CY, Harrison PH, Kwan TK. Pramanicin, an antifungal agent, raises cytosolic Ca^{2+} and causes cell death in vascular endothelial cells. *Vascul Pharm* 2003; **40**: 35–42.
3. Strasser A, O'Connor L, Dixit VM. Apoptosis signaling. *Annu Rev Biochem* 2000; **69**: 217–245.
4. Daniel PT. Dissecting the pathways to death. *Leukemia* 2000; **14**: 2035–2044.
5. Kaufmann SH, Earnshaw WC. Induction of apoptosis by cancer chemotherapy. *Exp Cell Res* 2000; **256**: 42–49.
6. Joza N, Kroemer G, Penninger JM. Genetic analysis of the mammalian cell death machinery. *Trends Genet* 2002; **18**: 142–149.
7. Kuida K, Boucher DM. Functions of MAP kinases: Insights from gene-targeting studies. *J Biochem (Tokyo)* 2004; **135**: 653–656.
8. Wada T, Penninger JM. Mitogen-activated protein kinases in apoptosis regulation. *Oncogene* 2004; **23**: 2838–2849.
9. Davis RJ. Signal Transduction to the nucleus by MAP Kinases in signaling networks and cell cycle control. In: Gutkind JS, ed. *The Molecular Basis of Cancer and Other Diseases*. Totowa, NJ: Humana Press 2000: 153–164.
10. Xia Z, Dickens M, Raingeaud J, *et al*. Opposing effects of ERK and JNK-p38 MAP kinases on apoptosis. *Science* 1995; **270**: 1326–1331.
11. Franklin RA, McCubrey JA. Kinases: Positive and negative regulators of apoptosis. *Leukemia* 2000; **14**: 2019–2034.
12. Liu ZG, Hsu H, Goeddel DV, *et al.* Dissection of TNF receptor 1 effector functions: JNK activation is not linked to apoptosis while NF-kappa B activation prevents cell death. *Cell* 1996; **87**: 565–576.
13. Lenczowski JM, Dominguez L, Eder AM, *et al.* Lack of a role for Jun kinase and AP-1 in Fas-induced apoptosis. *Mol Cell Biol* 1997; **17**: 170–181.
14. Rodrigues GA, Park M, Schlessinger J. Activation of the JNK pathway is essential for transformation by the Met oncogene. *EMBO J* 1997; **16**: 2634–2645.
15. Stofega MR, Yu CL, Wu J, *et al.* Activation of extracellular signal-regulated kinase (ERK) by mitogenic stimuli is

repressed in v-Src-transformed cells. *Cell Growth Differ* 1997; **8**: 113–119.
16. Ory S, Morrison DK. Signal transduction: Implications for Ras-dependent ERK signaling. *Curr Biol* 2004; **14**: R277–R278.
17. Duspara P, Jenkins SI, Hughes DW, *et al.* The biosynthesis of pramanicin: Intact incorporation of serine and absolute configuration of the antibiotic. *Chem Comm* 1998; **23**: 2643–2644.
18. Frelin C, Imbert V, Griessinger E, *et al.* AS602868, a pharmacological inhibitor of IKK2, reveals the apoptotic potential of TNF-alpha in Jurkat leukemic cells. *Oncogene* 2003; **22**: 8187–8194.
19. Kutuk O, Basaga H. Aspirin inhibits TNFalpha- and IL-1-induced NF-kappaB activation and sensitizes HeLa cells to apoptosis. *Cytokine* 2004; **25**: 229–237.
20. Pique M, Barragan M, Dalmau M, *et al.* Aspirin induces apoptosis through mitochondrial cytochrome*c* release. *FEBS Lett* 2000; **480**: 193–196.
21. Wang X, Martindale JL, Liu Y, *et al.* The cellular response to oxidative stress: Influences of mitogen-activated protein kinase signalling pathways on cell survival. *Biochem J* 1998; **333**: 291–300.
22. Viktorsson K, Ekedahl J, Lindebro MC, *et al.* Defective stress kinase and Bak activation in response to ionizing radiation but not cisplatin in a non-small cell lung carcinoma cell line. *Exp Cell Res* 2003; **289**: 256–264.
23. Schweyer S, Soruri A, Meschter O, *et al.* Cisplatin-induced apoptosis in human malignant testicular germ cell lines depends on MEK/ERK activation. *Br J Cancer* 2004; **91**: 589–598.
24. Giri DK, Pantazis P, Aggarwal BB. Cellular resistance to vincristine suppresses NF-kappa B activation and apoptosis but enhances c-Jun-NH2-terminal protein kinase activation by tumor necrosis. *Apoptosis* 1999; **4**: 291–301.
25. Harrison PHM, Duspara PA, Jenkins SI, *et al.* The biosynthesis of pramanicin in Stagonospora sp ATCC 74235: A modified acyltetramic acid. *J Chem Soc Perkin Trans I* 2000; **24**: 4390–4402.
26. Choi HJ, Lee SY, Cho Y, *et al.* JNK activation by tetrahydrobiopterin: Implication for Parkinson's disease. *J Neurosci Res* 2004; **75**: 715–721.
27. Hunot S, Vila M, Teismann P, *et al.* JNK-mediated induction of cyclooxygenase 2 is required for neurodegeneration in a mouse model of Parkinson's disease. *Proc Natl Acad Sci USA* 2004; **101**: 665–670.
28. Blaker H, Helmchen B, Bonisch A, *et al.* Mutational activation of the RAS-RAF-MAPK and the wnt pathway in small intestinal adenocarcinomas. *Scand J Gastroenterol* 2004; **39**: 748–753.
29. Tournier C, Hess P, Yang DD, *et al.* Requirement of JNK for stress-induced activation of the cytochrome *c* -mediated death pathway. *Science* 2000; **288**: 870–874.
30. Lin A, Dibling B. The true face of JNK activation in apoptosis. *Aging Cell* 2002; **1**: 112–116.
31. Mukundan L, Milhorn DM, Matta B, *et al*. CD40-mediated activation of vascular smooth muscle cell chemokine production through a Src-initiated, MAPK-dependent pathway. *Cell Signal* 2004; **16**: 375–384.
32. Wilson DJ, Alessandrini A, Budd RC. MEK1 activation rescues Jurkat T cells from Fas-induced apoptosis. *Cell Immunol* 1999; **194**: 67–77.
33. van den Brink MR, Kapeller R, Pratt JC, *et al.* The extracellular signal-regulated kinase pathway is required for activation-induced cell death of T cells. *J Biol Chem* 1999; **274**: 11178–11185.